

Strongly nonlinear magnetization above T_c in $\text{Bi}_2\text{Sr}_2\text{CaCu}_2\text{O}_{8+\delta}$

LU LI¹, YAYU WANG¹, M. J. NAUGHTON², S. ONO³, YOICHI ANDO³
and N. P. ONG¹

¹ *Department of Physics, Princeton University - NJ 08544, USA*

² *Department of Physics, Boston College - Chestnut Hill, MA 02467, USA*

³ *Central Research Institute of Electric Power Industry
Komae, Tokyo 201-8511, Japan*

received 26 July 2005; accepted 12 September 2005

published online 5 October 2005

PACS. 74.72.-h – Cuprate superconductors (high- T_c and insulating parent compounds).

PACS. 74.25.Ha – Magnetic properties of superconductors.

PACS. 74.25.Dw – Superconductivity phase diagrams.

Abstract. – Using high-resolution magnetometry we have investigated in detail the magnetization M above the critical temperature T_c in $\text{Bi}_2\text{Sr}_2\text{CaCu}_2\text{O}_8$. In a broad range of temperature T above T_c , we find that $M(T, H)$ is strongly non-linear in the field H . We show that as $T \rightarrow T_c$, the susceptibility $\chi(T, H)$ diverges to very large values ($\chi \rightarrow -1$) if measured in weak H . In addition, $M(H)$ displays an anomalous non-analytic form $M \sim H^{1/\delta}$ in weak fields with a strongly T -dependent exponent $\delta(T)$. These features strongly support the proposal that, above T_c , the pair condensate survives to support significant London rigidity.

Introduction. – The notion that superconductivity in the cuprates is destroyed by thermally created vortices has gained substantial experimental support. In single crystals, evidence for vortex excitations that persist above the critical temperature T_c to a temperature $T_{\text{onset}} \sim 120$ K has been obtained from the Nernst effect [1]. An enhanced diamagnetic signal that scales accurately as the Nernst signal has also been observed using high-field magnetometry [2]. These results reveal that, above T_c , significant pair-condensate amplitude survives up to intense magnetic fields H . Further, in ultra-thin films, the kinetic inductance has been observed to persist above T_c [3]. The sensitivity of superconductivity to phase fluctuations in cuprates has been investigated theoretically by several groups [4, 5].

In low- T_c superconductors, the condensate vanishes above T_c , except inside evanescent droplets created by amplitude (or Gaussian) fluctuations. The diamagnetic susceptibility χ from Gaussian fluctuations is very small ($\chi \sim 10^{-5}$) [6]. Given the vortex scenario in cuprates, the magnetization M measured above T_c ought to be qualitatively different from the Gaussian picture. However, resolving the signal in tiny crystals is very challenging, and the available results are confusing [7–10]. An experiment performed on aligned grains [7] claims agreement with the mean-field Gaussian theory. Other experiments are seemingly consistent with the vortex scenario, but uncover anomalies that are hard to interpret [8]. Here we report detailed measurements in $\text{Bi}_2\text{Sr}_2\text{CaCu}_2\text{O}_8$ (Bi 2212) showing that the weak-field susceptibility χ diverges exponentially consistent with Kosterlitz-Thouless (KT) behavior.

The strong nonlinearity observed in χ suggests the existence of a subtle rigidity in the pair wave function $\hat{\Psi}$ which persists above T_c .

Experimental details. – To cover a broad range of fields, we have combined torque magnetometry with SQUID magnetometry. In the torque experiment, the crystal is glued at the tip of the Si cantilever beam with its c -axis at a tilt angle $\varphi \simeq 15^\circ$ to \mathbf{H} . In our experiment, the torque $\vec{\tau}$ is the sum of a paramagnetic term from the spin moment \mathbf{m}_p and a diamagnetic term from the magnetization \mathbf{M} of interest here, *viz* $\vec{\tau} = [\mathbf{m}_p + V\mathbf{M}] \times \mu_0\mathbf{H}$, with V the sample volume and μ_0 the permeivity. For temperatures $T > T_c$, \mathbf{M} is strictly along the z -axis (we take $\hat{\mathbf{z}}||\hat{\mathbf{c}}$). An in-plane component M_x is resolvable only below the irreversibility line [11] (from hereon, $M_z = M$). We define the effective magnetization $M_{eff} \equiv \tau/(\mu_0 H_x V)$ where $H_x = H \sin \varphi$. For $\varphi \ll 1$, we have

$$M_{eff}(T, H) = \Delta\chi_p H_z + M(T, H_z), \quad (1)$$

where the anisotropy $\Delta\chi_p = \chi_c - \chi_a$ is the difference between the c -axis and in-plane spin susceptibilities. As explained in ref. [2], the very weak T -dependence of $\Delta\chi_p$ in cuprates allows the strongly T -dependent $M(T, H)$ to be extracted reliably from M_{eff} . All curves reported here are *fully reversible* (hystereses caused by pinning of vortices are only seen below ~ 50 K). We studied 2 slightly underdoped (UD) Bi 2212 crystals with $T_c = 86$ and 85 K (samples I and II) with very similar results.

If M is nearly linear in H (valid if $T > 1.1 T_c$ and $H > 0.5$ T), eq. (1) implies that the torque varies sinusoidally, *viz* $\tau/V = \mu_0(\Delta\chi_p - \chi)H_x H_z \equiv A_1 \sin 2\varphi$, where $A_1(T, H) \sim H^2$ and changes sign above T_c , as observed in cuprates [11] (see below).

Magnetization and susceptibility. – First, we discuss the curves of $M(H)$ below T_c . The curves of $M(H)$ in fig. 1 were measured by SQUID magnetometry. Much analysis has focussed

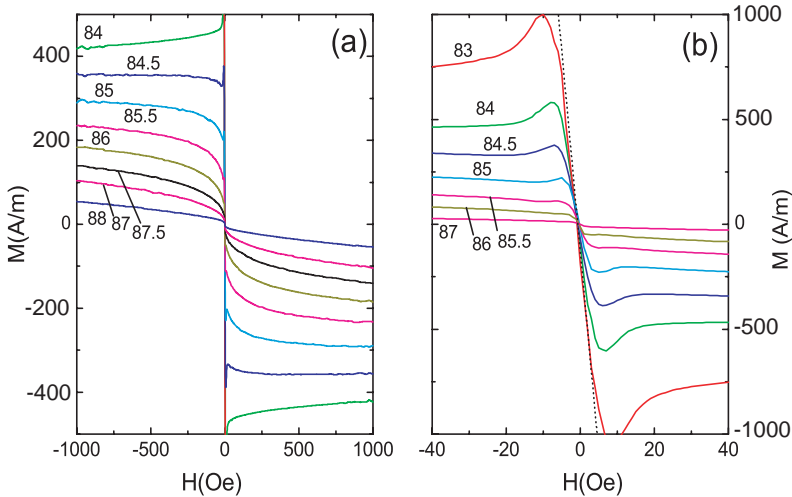


Fig. 1 – Magnetization M vs. H measured in sample 1 in fields $|H| < 1000$ Oe (panel (a)) and in fields $|H| < 40$ Oe (b). M is measured in the SQUID magnetometer in the long-time averaging mode (~ 12 h per curve). In panel (a), the sharp notch near $H = 0$ for $T < T_c$ ($= 86$ K) is H_{c1} . These features are shown more clearly in panel (b) with a 25-fold expansion in the field scale. The dotted line is $M/H = \chi/(1 + N_c\chi) = 2.55$ with $\chi = -0.95$ and $N_c = 0.64$ for sample I with $\mathbf{H}||\hat{\mathbf{c}}$. The peaks locate H_{c1} .

on the curve of $M(H)$ at the “crossing temperature” T_s ($= 84$ K) at which $M(H)$ is very nearly H -independent. By detecting the flux-exclusion in very weak fields, we have determined that the 3D transition at T_c (86 K) actually lies 2 K above T_s . In the interval T_s – T_c , a prominent anomaly of the curves of $M(H)$ is that they curve steeply towards zero as $H \rightarrow 0$ even though full flux exclusion obtains when $H < H_{c1}$ (the lower critical field). This feature may be seen in earlier reports on M [12], but has not received comment. Closer inspection reveals that $M(H)$ displays a notch feature which we show in expanded scale in fig. 1b. The notch corresponds to the initial entry of vortices at H_{c1} . Below H_{c1} , flux exclusion gives a linear M - H variation with a steep slope given by $M/H = \chi/(1 + N_c\chi)$, where $N_c \simeq 0.64$ is the demagnetization factor. Taking $\chi = -0.95$, we have $M/H = -2.55$ which is plotted as the broken line in fig. 1b. Both the full flux-exclusion implied by $\chi \sim -1$ and the sharp onset are evidence for a high degree of electronic homogeneity and uniformity of the condensate.

In low- T_c superconductors, $|M|$ falls steeply above H_{c1} , and continues its monotonic decrease until H attains the upper critical field H_{c2} . Here, the behavior is qualitatively different. Just above H_{c1} , $|M(H)|$ falls to a minimum, but then slowly increases over several decades in H . Following the initial entry of vortices, the sample steadily becomes *more diamagnetic* with increasing B . As we show, this paradoxical pattern reflects the phase-disordering nature of the transition at T_c in hole-doped cuprates.

We turn next to temperatures above T_c , where the resolution of the torque cantilever ($\sim 10^{-9}$ emu at 10 T) allows M to be studied in detail. Figure 2 displays the H -dependence of M at temperatures increasing from near T_c to 100 K. Over this broad interval, M increases with H with a curvature that becomes increasingly pronounced near T_c . These curves are strikingly similar to those in the interval T_s – T_c , except for the conspicuous absence of the notch feature associated with a finite H_{c1} .

We may combine the SQUID and torque results over our full field and temperature range in fig. 3. The SQUID results cover the low- H regime (10 Oe to 1000 Oe) while the torque curves extend to much higher fields. In this combined plot, M initially increases as a power law in H , reaches a broad maximum at fields 1–10 T and then decreases monotonically. The fan-like dispersion of the straight lines in low fields implies that M has the power-law behavior

$$M(T, H) = A(T)H^{1/\delta(T)} \quad (H \rightarrow 0), \quad (2)$$

described by a strongly T -dependent exponent $\delta(T)$ (A is field independent). In the interval 84–105 K, where $\delta > 1$, the non-analytic form of M implies that, as $H \rightarrow 0$, the diamagnetic susceptibility increasingly exceeds linear-response behavior (dashed line drawn for 87 K).

In fig. 4, the susceptibility $\chi(T, H) \equiv M(T, H)/H$ is displayed *vs.* T , with H as the parameter. Evidently, $\chi(T, H)$ is highly sensitive to H especially near T_c . If χ is measured at a fixed H , say 0.5 T, it stays non-divergent across T_c . However, this is not intrinsic. Instead, from 105 to 86 K, $|\chi|$ measured in a very weak field increases by 5 decades to attain values 0.1–1 just above T_c . As discussed later, this steep increase reflects a rapidly changing phase correlation length.

Previous experiments on “fluctuation diamagnetism” in cuprates failed to observe a divergent χ because the H applied was too large [7, 8, 10]. The strong H -dependence in $\chi(T, H)$ now call their conclusions into question. Further, vortex pinning effects, especially strong in polycrystalline samples of $\text{La}_{2-x}\text{Sr}_x\text{CuO}_4$ and $\text{YBa}_2\text{Cu}_3\text{O}_{7-\delta}$, introduce extrinsic features in M which render analyses problematical.

KT correlation length. – There are 2 major aspects of the non-linearity in $M(T, H)$ above T_c . The first reflects the divergent growth of the phase correlation length $\xi(T)$ while the second is the singular behavior in eq. (2). The 2D phase correlation length measures the

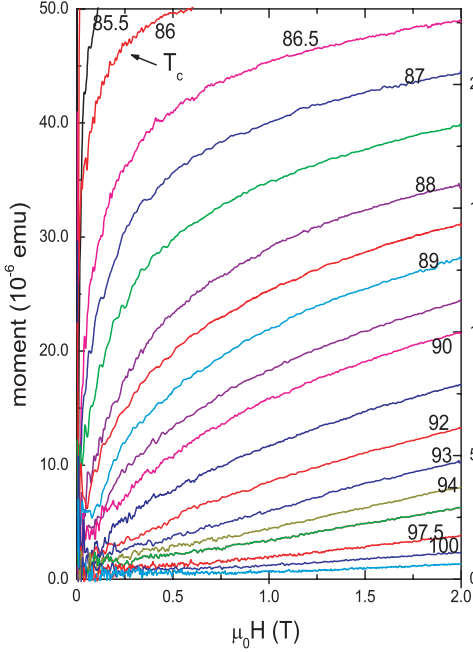


Fig. 2

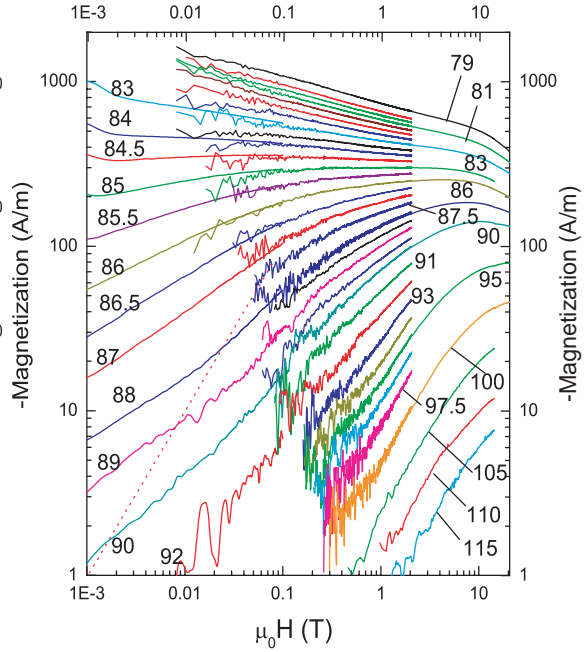


Fig. 3

Fig. 2 – Curves of M vs. H in Bi 2212 (sample I) measured by torque magnetometry for T above $T_c = 86$ K. The pronounced curvature evident in fig. 1a persists to ~ 100 K in fields up to 2 T and higher. The maximum beam deflection angle $\delta\varphi$ is 0.15° , or $10^{-2}\varphi$.

Fig. 3 – The field dependence of $M(T, H)$ in Bi 2212 ($T_c = 86$ K) from $H = 10$ Oe to 20 T at $T = 79$ –115 K (sample I). The log-log plot shows that $M(H)$ obeys eq. (2) as $H \rightarrow 0$. The slight upturn at 83 and 84 K near 10 Oe reflects H_{c1} (fig. 1b). The plot combines SQUID results (10 to 1000 Oe) and torque magnetometry results (500 Oe to 2 T). Torque results up to 20 T are also shown at selected T . The dashed line (of slope 1) is the linear response of eq. (3) at 87 K.

region within which phase coherence prevails in each layer. In KT theory long-range phase coherence is destroyed by the appearance of (anti) vortices at the KT transition (at T_{KT}). Hence the KT correlation length ξ_{KT} is the average spacing between these thermally created vortices. Above T_{KT} , $M(T, H)$ is linear in H in low fields. The weak-field susceptibility is [13]

$$\chi_{KT} = -\frac{\mu_0 k_B T}{2d\phi_0^2} \xi_{KT}^2 \quad (T > T_{KT}, H \rightarrow 0), \quad (3)$$

where k_B is Boltzmann's constant, d the bilayer spacing, and ϕ_0 the superconducting flux quantum. The KT correlation length is exponential in the reduced temperature $t' = T/T_{KT} - 1$, viz $\xi_{KT} = ae^{b/\sqrt{t'}}$, with $b \sim 1$ a non-universal constant and a a cut-off length \sim the vortex core size.

Clearly, an interlayer coupling J_\perp needs to be included to describe the actual 3D transition at T_c (see below). Nonetheless, the KT theory describes the essential features of a divergent $\xi(T)$ and the roles of thermally induced vs. field-induced vortices in each layer. In fig. 4, the dashed curve is a fit of eq. (3) with $b = 1.0$ and $a = 10 \text{ \AA}$. The fit captures quantitatively the broad features of the 5-decade rise in $\chi(T, H)$ in weak H , matching its curvature both near T_c and near 100 K.

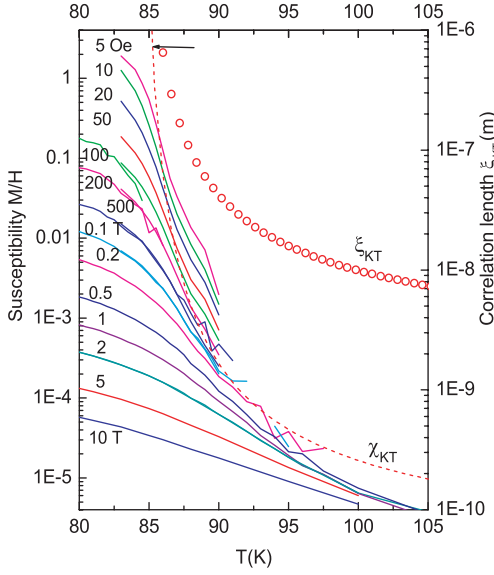


Fig. 4

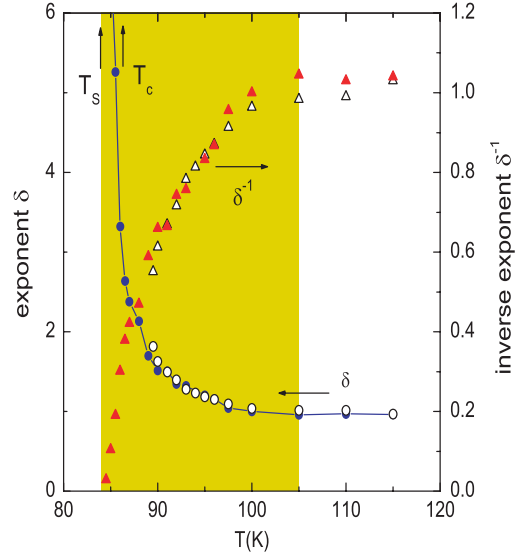


Fig. 5

Fig. 4 – The temperature and field dependence of the susceptibility $\chi(T, H) = M(T, H)/H$. In weak H , $|\chi|$ increases by over 5 decades from 100 K to T_c , reaching the full flux-expulsion value (enhanced by demagnetization) shown by the arrow. The dashed curve is a fit to eq. (3) with $b = 1$, $d = 12 \text{ \AA}$, $a = 10 \text{ \AA}$, and $T_{KT} = 84 \text{ K}$. Open circles represent the KT correlation length ξ_{KT} obtained from the fit.

Fig. 5 – The T -dependence of the weak-field magnetization exponent $\delta(T)$ in samples I (solid circles) and II (open circles). The reciprocal $\delta(T)^{-1}$ is plotted as solid and open triangles for I and II, respectively. As $T \rightarrow T_s^+$, $\delta(T)^{-1}$ decreases smoothly to 0. In the shaded region from T_s to 105 K, where $\delta > 1$, linear magnetic response is absent even at 10 Oe (eq. (2)).

The KT correlation length ξ_{KT} inferred from the fit increases from $\sim 8 \text{ nm}$ at 105 K to 700 nm at 86 K. A second length scale is the spacing $a_B = \sqrt{\phi_0/B}$ of vortices inserted by \mathbf{H} . To observe the intrinsic divergence in ξ_{KT} , we need $a_B \gg \xi_{KT}$ or $B \ll B_{th}$, where $B_{th} \equiv \phi_0/\xi_{KT}^2$ is a field-scale set by the density of thermally created (anti)vortices. As $T \rightarrow T_s$ in a fixed field $B \ll B_{th}$, $\chi(T)$ initially increases rapidly (and B_{th} decreases). However, χ saturates to a constant when B_{th} approaches B , as evident for the curves in fig. 4.

Singular response as $H \rightarrow 0$. – Despite the reasonable fit to $\chi(T)$, eq. (3) does not account for the non-analytic behavior expressed in eq. (2). As mentioned, the deviation between $M(H)$ at 87 K and the dashed line in fig. (3) grows as H decreases. We now discuss in more detail the T -dependence of this non-analyticity. From 105 K to 84 K, the weak-field slopes in the log-log plots in fig. 3 decrease smoothly from ~ 1 to zero, *i.e.* $\delta(T)$ diverges to values exceeding 20. The steepness of this increase is evident in the plots in fig. 5 for samples I and II (solid and open circles, respectively). The *continuous* nature of the increase in $\delta(T)$ is made clearer by plotting its reciprocal, which falls below 1 and smoothly approaches 0 as $T \rightarrow T_s^+$ (triangles). In fig. 5, the shading highlights the interval from T_s to $\sim 105 \text{ K}$ in which δ exceeds 1. In the shaded interval above T_c , χ diverges steeply in the limit $H \rightarrow 0$ assuming eq. (2) remains valid. Hence, despite the absence of a true Meissner state, a feeble H induces a large diamagnetic screening current. Below T_c , however, this limit is interrupted at H_{c1} by the appearance of the Meissner state, as discussed in fig. 1b.

Generally, the Meissner state originates from the rigidity of the pair wave function $\hat{\Psi}$. In a field, this “London rigidity” suppresses the paramagnetic current response, leaving only the full diamagnetic current [14]. Here, our magnetization results imply that, despite the loss of the Meissner effect, $\hat{\Psi}$ retains some rigidity above T_c . However, the rigidity is very fragile and observable only in a feeble field. The existence of a singular diamagnetic response above T_c has not been predicted (for, *e.g.*, δ is strictly 1 above T_{KT} in KT theory). Singular behavior in the weak-field vortex-liquid response is discussed in ref. [15].

Discussion. – We now return to the anomalous behavior of $M(H)$ in the interval T_s – T_c where full flux-exclusion prevails for $H < H_{c1}$. As mentioned, the curves below T_c closely resemble those above (compare figs. 1a and 2). Aside from fields below H_{c1} , the curves of M in the log-log plot in fig. 3 assume a fan-like dispersion that smoothly extends the behavior in this interval to above T_c . The exponent $1/\delta(T)$, which measures the slopes, continuously decreases across T_c (fig. 5). This continuity strongly implies that the anomalous magnetization in the 2 K interval below T_c and above T_c share the same origin; both represent the diamagnetic response of a strongly phase-disordered 2D superconducting state with a very high depairing field $H_{c2} > 80$ T [2]. Between T_s and T_c , the magnetization is comprised of a weak-field 3D Meissner state that pre-empts the phase-ordering transition of the 2D condensate at T_s . Application of $H > H_{c1}$ destroys the Meissner state and uncovers the underlying 2D state whose magnetization continues to grow with field. This accounts for the unusual “minimum” in $|M|$ just above H_{c1} mentioned in fig. 1a. The steep fall of $|M|$ just above H_{c1} reflects the destruction of the 3D Meissner state, while the subsequent power law increase reflects the behavior of M in the underlying 2D condensate which is robust to intense fields.

A hint of our results may be seen in previous torque experiments [9, 11]. In crystals of $Tl_2Ba_2CuO_{6+\delta}$ with $T_c = 25$ and 15 K, the measured curve of τ vs. φ displays a puzzling, unexpected term $A_1 \sin 2\varphi$ which is actually dominant above T_c [11]. Using eq. (1) and our analysis, we now understand this term to be the robust 2D magnetization which persists to intense H and high T as discussed above. As noted, the rapid decrease in $|M|$ above T_c , compared with the mild change in $\Delta\chi_p$, engenders a sign change in $A_1(T, H)$ as seen (fig. 5 in ref. [11]).

The transition in cuprates has been frequently compared to the 3DXY transition with large anisotropy α^{-1} , where $\alpha = J_{\perp}/J$ with J the intralayer coupling and J_{\perp} the interlayer coupling [16, 17]. Our findings that the KT theory gives a broadly accurate description of $\chi(T, H)$ and that $T_c - T_{KT} \sim 2$ K $\ll T_c$ confirm that Bi 2212 falls in the extreme limit $\alpha \ll 1$. (By way of comparison, in the planar ferromagnet K_2CuF_4 with $\alpha \ll 1$, the KT theory also describes well M vs. H above its Curie temperature T_C [18]. However, the 3D transition $T_C = 6.25$ K pre-empts the 2D KT transition ($T_{KT} \sim 5.6$ K) [18, 19]. Below T_c , the destruction of the 3D Meissner state here obviously has no parallel in the planar magnet.) Unfortunately, the limit $\alpha \ll 1$ is intractable analytically. Currently, numerical simulations of M on lattices [16, 17] do not seem to have sufficient resolution to fit the measurements meaningfully.

At T_c , the phase of $\hat{\Psi}$ is strongly disordered by vortex motion. However, the continued growth of these signals to intense fields (30–45 T) implies that the depairing field H_{c2} lies much higher (80–100 T). Below ~ 105 K, the non-linear behavior of χ becomes increasingly apparent. In weak H , $\chi(T, H)$ undergoes a 5-decade increase as T_c is approached, whose broad features can be understood in terms of a diverging phase-correlation length ξ , as prescribed in KT theory (fig. 4). In the shaded interval in fig. 5, χ is further enhanced by a singular power law dependence suggestive of increasing London rigidity.

Lastly, the singular, non-Gaussian nature of the diamagnetic fluctuations explains why early “fluctuation conductivity” data [20] were poorly described by Gaussian theory (Aslamasov-Larkin and Maki-Thompson terms), especially in large H in the UD regime.

* * *

We acknowledge valuable discussions with V. OGANESYAN, S. SONDHI, V. MUTHUKUMAR and P. W. ANDERSON. The research is supported by U.S. National Science Foundation (NSF) through a MRSEC grant DMR 0213706 and by the Grant-in-Aid for Science provided by the Japan Society for the Promotion of Science. Some measurements were done at the National High Magnetic Field Laboratory, Tallahassee, which is supported by NSF and the State of Florida.

REFERENCES

- [1] XU Z. A., ONG N. P., WANG Y., KAKESHITA T. and UCHIDA S., *Nature*, **406** (2000) 486; WANG Y. *et al.*, *Phys. Rev. B*, **64** (2001) 224519; WANG Y. *et al.*, *Phys. Rev. Lett.*, **88** (2002) 257003; WANG Y. *et al.*, *Science*, **299** (2003) 86; CAPAN C. *et al.*, *Phys. Rev. Lett.*, **88** (2002) 056601; WEN H. H. *et al.*, *Europhys. Lett.*, **63** (2003) 583.
- [2] WANG Y., LI L., NAUGHTON M. J., GU G. D., UCHIDA S. and ONG N. P., cond-mat/0503190.
- [3] CORSON J. *et al.*, *Nature*, **398** (1999) 221.
- [4] EMERY V. J. and KIVELSON S. A., *Nature*, **374** (1995) 434.
- [5] GESHKENBEIN V. B., IOFFE L. B. and LARKIN A. I., *Phys. Rev. B*, **55** (1997) 3173; FRANZ M. and MILLIS A. J., *Phys. Rev. B*, **58** (1998) 14572; BASKARAN G. *et al.*, *Solid State Commun.*, **63** (1987) 973; HONERKAMP C. and LEE P. A., *Phys. Rev. Lett.*, **92** (2004) 177002.
- [6] GOLLUB J. P., BEASLEY M. R. and TINKHAM M., *Phys. Rev. Lett.*, **25** (1970) 1646.
- [7] CARBALLEIRA C., MOSQUEIRA J., REVCOLEVSKI R. and VIDAL F., *Phys. Rev. Lett.*, **84** (2000) 3157.
- [8] CARRETTA P. *et al.*, *Phys. Rev. B*, **61** (2000) 12420.
- [9] NAUGHTON M. J., *Phys. Rev. B*, **61** (2000) 1605.
- [10] LASCIALFARI A. *et al.*, *Phys. Rev. B*, **65** (2002) 144523; LASCIALFARI A. *et al.*, *Phys. Rev. B*, **68** (2003) 100505.
- [11] BERGEMANN C. *et al.*, *Phys. Rev. B*, **57** (1998) 14387.
- [12] KES P. *et al.*, *Phys. Rev. Lett.*, **67** (1991) 2383; WELP U. *et al.*, *Phys. Rev. Lett.*, **67** (1991) 3180.
- [13] OGANESYAN V., HUSE D. A. and SONDHI S. L., cond-mat/0502224.
- [14] SCHRIEFFER J. R., *Theory of Superconductivity* (Addison Wesley) 1964, Chapt. 8.
- [15] ANDERSON P. W., cond-mat/0504453.
- [16] JANKE W. and MATSUI T., *Phys. Rev. B*, **42** (1990) 10673.
- [17] NGUYEN A. K. and SUDBØ A., *Phys. Rev. B*, **60** (1999) 15307.
- [18] HIRAKAWA K. and UBUKOSHI K., *J. Phys. Soc. Jpn.*, **50** (1981) 1909.
- [19] HIKAMI S. and TSUNETO T., *J. Phys. Soc. Jpn.*, **63** (1980) 387.
- [20] SEMBA K., ISHII T. and MATSUDA A., *Phys. Rev. Lett.*, **67** (1991) 2114; SEMBA K. and MATSUDA A., *Phys. Rev. B*, **55** (1997) 11103.